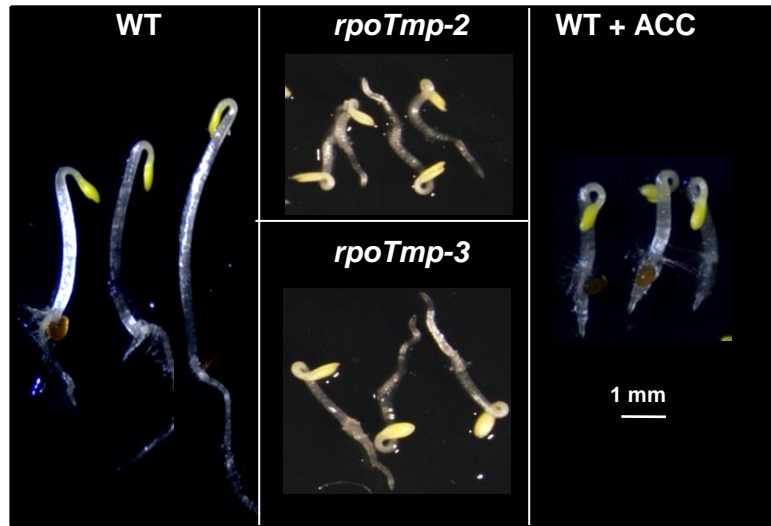
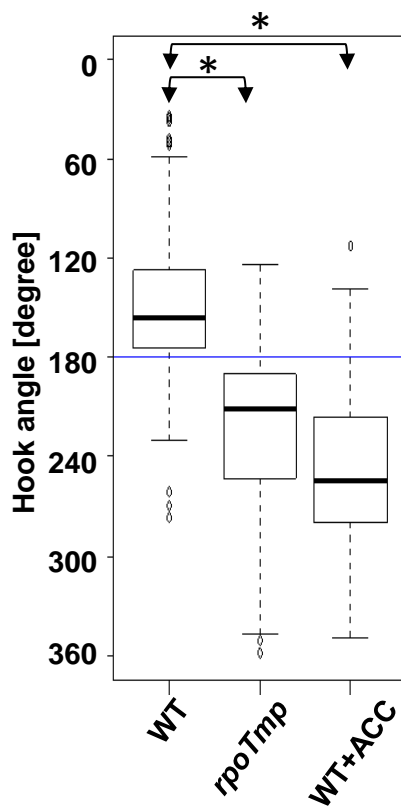


a



b



c

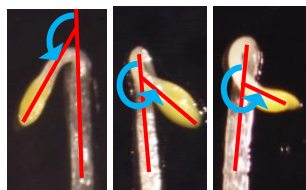
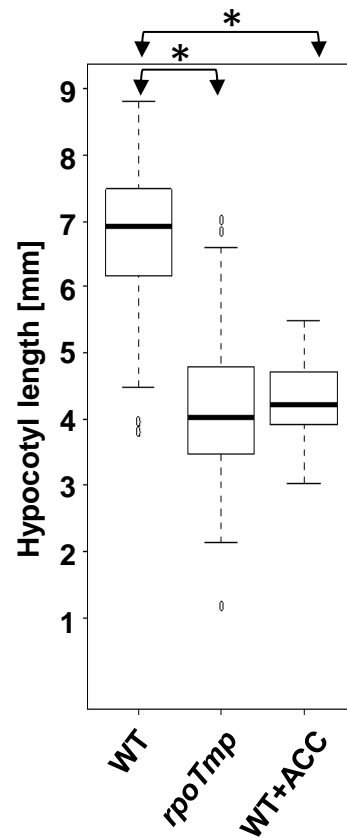
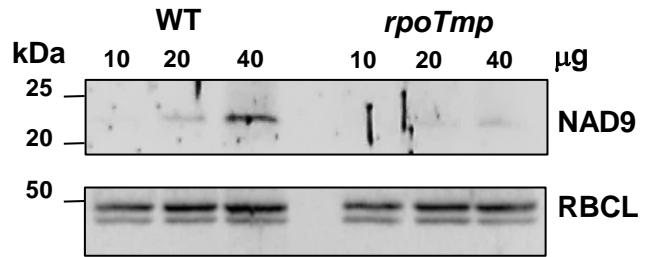


**Fig. 1 Etiolated *rpoTmp* mutant plantlets exhibit a triple-response-like phenotype.** **a)** Images of etiolated *rpoTmp* mutant (two mutant alleles, *rpoTmp-2* SALK\_132842 and *rpoTmp-3* SALK\_086115) and WT plants (grown in presence or in absence of 20 mM ACC) were taken under a dissection microscope. Scale bar corresponds to 1 mm. **(b)** Top panel: Median values of apical hook angle measurements were box-plotted for WT plants grown in absence or in presence of 20  $\mu$ M ACC and for *rpoTmp* plants. The number of pooled individuals (N) that were measured in 7 independent hook angle analyses corresponds to 304 for WT plants; N (measured in 3 independent analyses) corresponds to 130 for WT + ACC plants; N (measured in 5 independent analyses) corresponds to 211 for *rpoTmp* plants. Data are box-plotted using versions of the first and third quartiles [27] with median values (horizontal lines inside the box). The external horizontal lines show the largest or smallest observations that fall within a distance of 1.5 times the box size from the nearest hinge. Additional points are extreme value observations. The asterisks (\*) indicate significant difference between two samples. Bottom panel: Principle of angle determination. Magnified images of the hook from WT, *rpoTmp* and ACC-treated WT. The apical hook curvature was measured as the angle (blue line) that is formed by the two straight lines (red) passing through the hypocotyl and the cotyledon axes. Any hook angle larger than 180° (blue horizontal line) was considered as twisted. Images were analyzed with the ImageJ programme. **(c)** Median values of hypocotyl length measurements were box-plotted for WT plants grown in absence or in presence of 20  $\mu$ M ACC and for *rpoTmp* plants. N (measured in 2 independent analyses) corresponded to 92 for WT plants; to 75 for ACC-treated WT plants; to 98 for *rpoTmp* plants. Data are box-plotted as in **Fig.1b**.

a

Gene	<i>rpoTmp</i> /WT log2FC	BH adj P-value	Protein
atmg00070	-0,31	0,12	NAD9
atmg00210	-0,33	0,14	RPL5
atmg00270	-2,14	0,00	NAD6
atmg00285	-0,76	0,00	NAD2A
atmg00290	-1,45	0,00	RPS4
atmg00513	-0,84	0,00	NAD5A
atmg00516	-0,43	0,04	NAD1C
atmg00580	-0,53	0,01	NAD4
atmg01360	-0,86	0,00	COX1

b

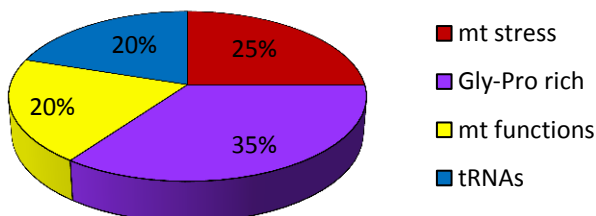


c

Gene	<i>rpoTmp</i> /WT log2FC	BH adj. P-value	Protein	Mt localization	Function
at5g09570	4,19	1,40E-05	AT12CYS-2, Twin Cysteine Protein	mt	Mt stress
at1g55990	3,18	4,13E-03	glycine-rich protein		Gly-Pro rich
at1g64220	2,83	1,33E-03	TOM7-2, translocase of outer membrane 7 kda subunit 2)	mt	Mt functions
at5g09520	2,73	3,61E-03	hydroxyproline-rich glycoprotein family protein		Gly-Pro rich
at2g20800	2,67	9,50E-04	NDB4, external alternative NAD(P)H dehydrogenase	mt	Mt stress
at5g54100	2,67	3,32E-05	SLP2, protein phosphatase	mt	Mt functions
atmg00190	2,58	1,85E-06	TRNG, tRNA-Gly	mt	tRNA
at5g54560	2,50	4,90E-03	ATDOB13, protein of unknown function (DUF 295)	mt	Mt stress
at1g60050	2,50	1,66E-02	Nodulin MtN21 /EamA-like transporter family protein		Gly-Pro rich
at5g52940	2,49	7,33E-04	ATDOB5, protein of unknown function (DUF 295)	mt	Mt stress
atmg00250	2,42	6,82E-05	TRNM.1, tRNA-Met	mt	tRNA
at2g24980	2,39	2,15E-02	Proline-rich extensin-like family protein		Gly-Pro rich
at5g13900	2,36	5,14E-03	seed storage 2S albumin superfamily protein		Gly-Pro rich
at4g33610	2,28	1,24E-02	glycine rich protein		Gly-Pro rich
atmg00630	2,21	1,23E-04	ORF 110B, hypothetical protein	mt	Mt functions
at5g54450	2,21	2,27E-03	ATDOB11, , protein of unknown function (DUF 295)	mt	Mt stress
at5g09530	2,20	1,68E-02	hydroxyproline rich protein		Gly-Pro rich
at2g07745	2,18	6,96E-03	pre-tRNA		tRNA
atmg01340	2,16	2,44E-04	TRNM.2, tRNA-Met	mt	tRNA
at2g07777	2,14	1,12E-04	ATP synthase 9	mt	Mt functions

d

## Top 20 up-regulated genes



e

## Top 20 down-regulated genes

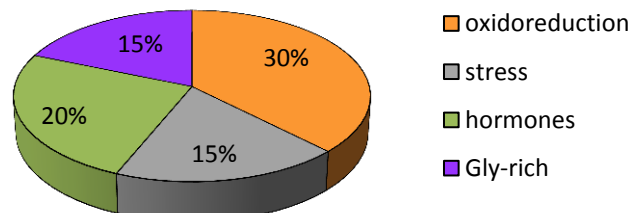


**Fig. 2 Relative gene expression profiles of *rpoTnp* mutants versus WT etiolated plants.** **a)** The relative expression values for the RPOtnp-dependent sub-set of mitochondrial genes are indicated in the middle panel together with the corresponding P-values, which are derived from a t-test adjusted for false discovery rate (FDR) after the Benjamini-Hochberg (BH) procedure. Gene identities are indicated in the left, and protein identities in the right panels. Given values represent log<sub>2</sub>-fold changes (FC). **b)** Analysis of accumulation of NAD9 protein, used as marker for complex I accumulation. Protein extracts (10, 20, 40 µg) from etiolated WT and *rpoTnp* plants were fractionated and immunoblotted with specific antisera against the mitochondrial proteins NAD9 (mitochondrial-encoded) and the plastidial proteins RBCL (plastidial-encoded). **c)** Relative expression values for the 20 most up-regulated genes in *rpoTnp* plants. Details as in **a)**. Mitochondrial (mt) localization and protein function are also indicated on the right side of the table. “Mt stress” stands for “response to mitochondrial stress”. **d)** Functional sub-grouping of the 20 most up-regulated genes listed in **c)**. The four groups identified were color-coded as in **c)**. For details see text. **e)** Functional sub-grouping of the 20 most down-regulated genes (**Table S4**). The four groups identified were color-coded as in **c)**. The terms “hormones” and “stress ” for protein functions stand for “response to hormonal stimuli” and “response to stress”, respectively.

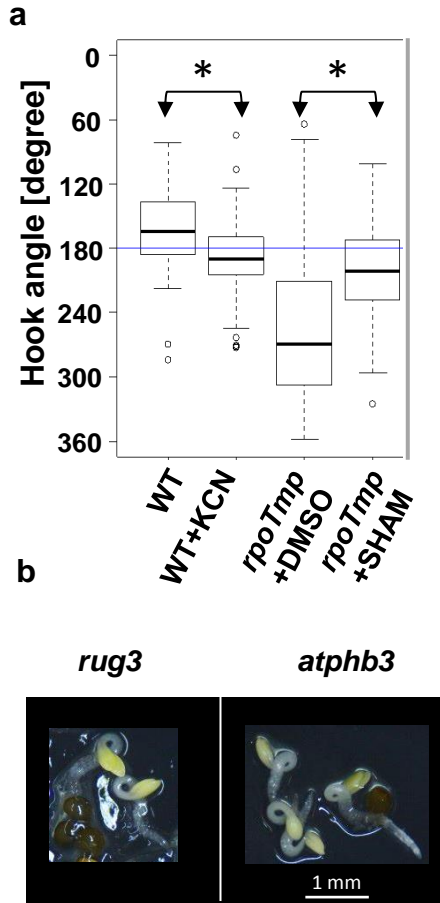


**Fig. 3 Plants that are defective in respiration present a triple-response-like phenotype.** **a)** Median values of apical hook angle measurements were box-plotted for WT plants that were grown in presence of 1 mM KCN or H<sub>2</sub>O as mock-control and mutant *rpoTmp* plants that were grown in presence of 1 mM SHAM or DMSO as mock-control. N (measured in four independent analyses) corresponds to 178 for H<sub>2</sub>O-treated WT plants and to 128 for KCN-treated WT plants. N (measured in two independent analyses) corresponds to 148 for DMSO-treated *rpoTmp* plants and to 85 for SHAM-treated *rpoTmp* plants. Details of box-plot representation are explained in **Fig. 1b**. **b)** Images of etiolated mutant *rug3* and *atphb3* plants were taken under a dissection microscope. Scale bar corresponds to 1 mm.

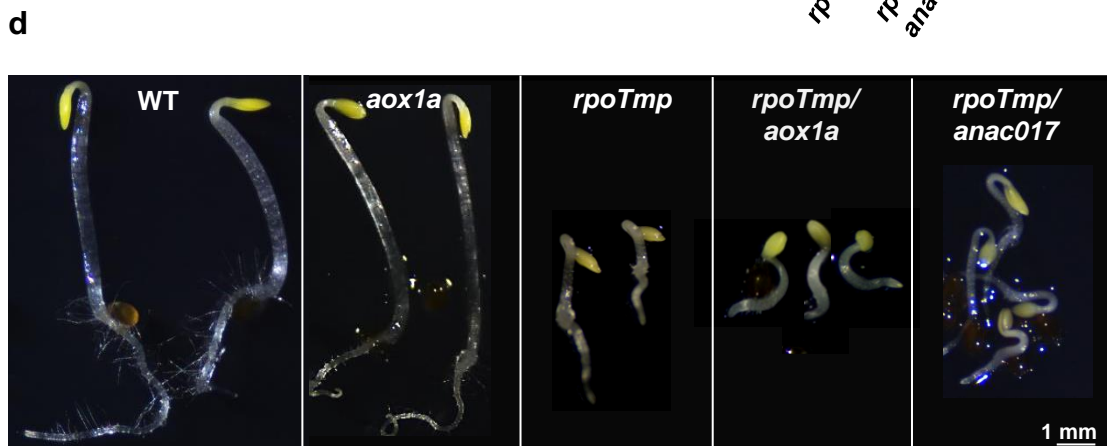
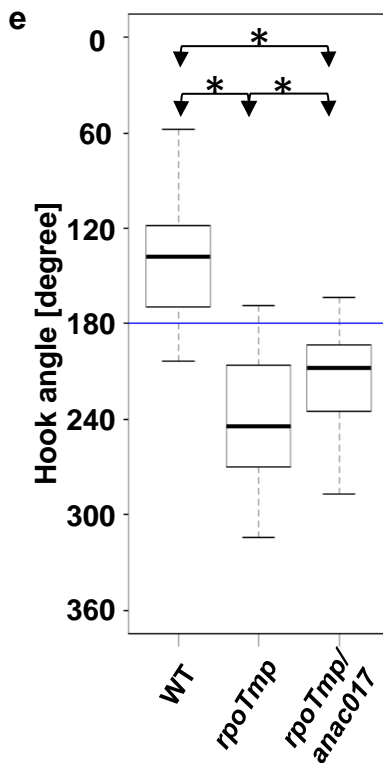
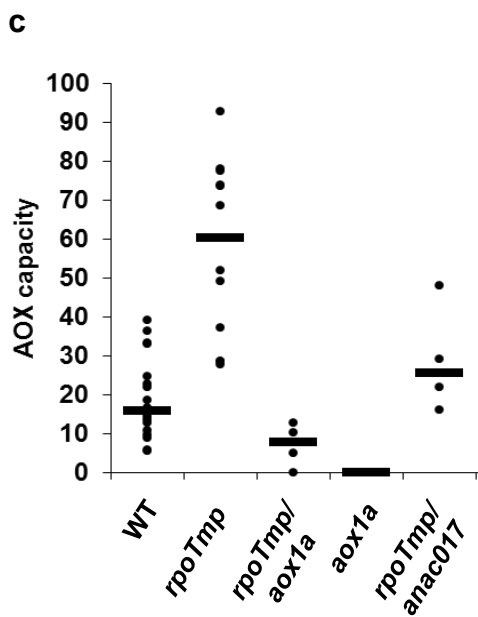
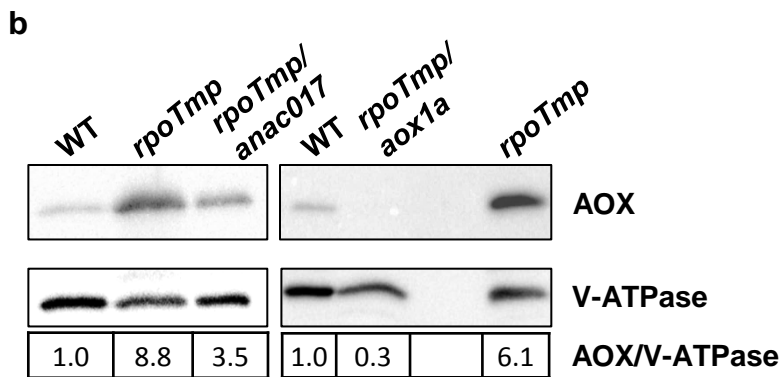
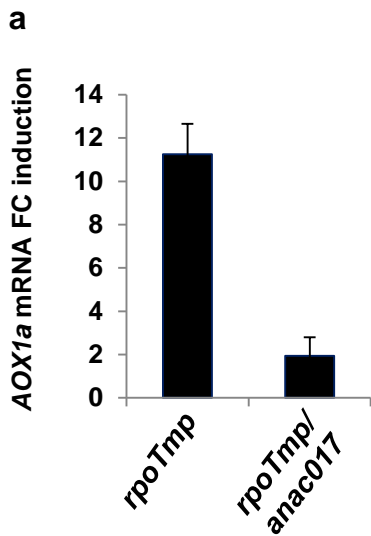


**Fig. 4 The triple-response-like phenotype in *rpoTmp* mutant plants requires AOX1a.** **a)** Linear fold change (FC) induction of *AOX1a* mRNAs in mutant *rpoTmp* and *rpoTmp/anac017* plants versus WT determined by RT-qPCR. The *AOX1a* expression levels were normalized with the mean of *ACTIN2-8* expression, used as reference gene. The mean values of two biological replicates are plotted. Error bars correspond to standard errors. **b)** Protein extracts from etiolated WT, *rpoTmp*, *rpoTmp/anac017* plants (left panel) and WT, *rpoTmp/aox1a*, *rpoTmp* plants (right panel) were fractionated and immunoblotted with specific antisera against the mitochondrial AOX isoforms and the vacuolar protein as loading control. Linear fold change variation of AOX protein levels in mutant *rpoTmp* plants versus WT using V-ATPase for normalization is described in the table (bottom panel). **c)** Capacity of the AOX-dependent pathway in etiolated mutant plants. AOX capacity was calculated upon addition of 1 mM KCN into the measurement cell (final concentration). The figure presents the ratio in percentage of the KCN-insensitive O<sub>2</sub> consumption rate to the total consumption rate. Median values (thick horizontal lines) of N independent measurements (full circles) were scatter-plotted for WT (N=19), *rpoTmp* (N=12), *rpoTmp/aox1a* (N=5), *aox1a* (N=4) and *rpoTmp/anac017* plants (N=4). **d)** Images of etiolated plants: WT, *aox1a*, *rpoTmp*, *rpoTmp/aox1a*, *rpoTmp/anac017* were taken under a dissection microscope. Scale bar corresponds to 1 mm. **e)** Median values of apical hook angle measurements are box-plotted for WT, mutant *rpoTmp* and *rpoTmp/anac017* plants. Values were measured in 2 independent analyses. N =53 for WT plants; N =57 for *rpoTmp* plants; N= 57 for *rpoTmp/anac017* plants. Details of box-plot representation are as given in Fig. 1b.

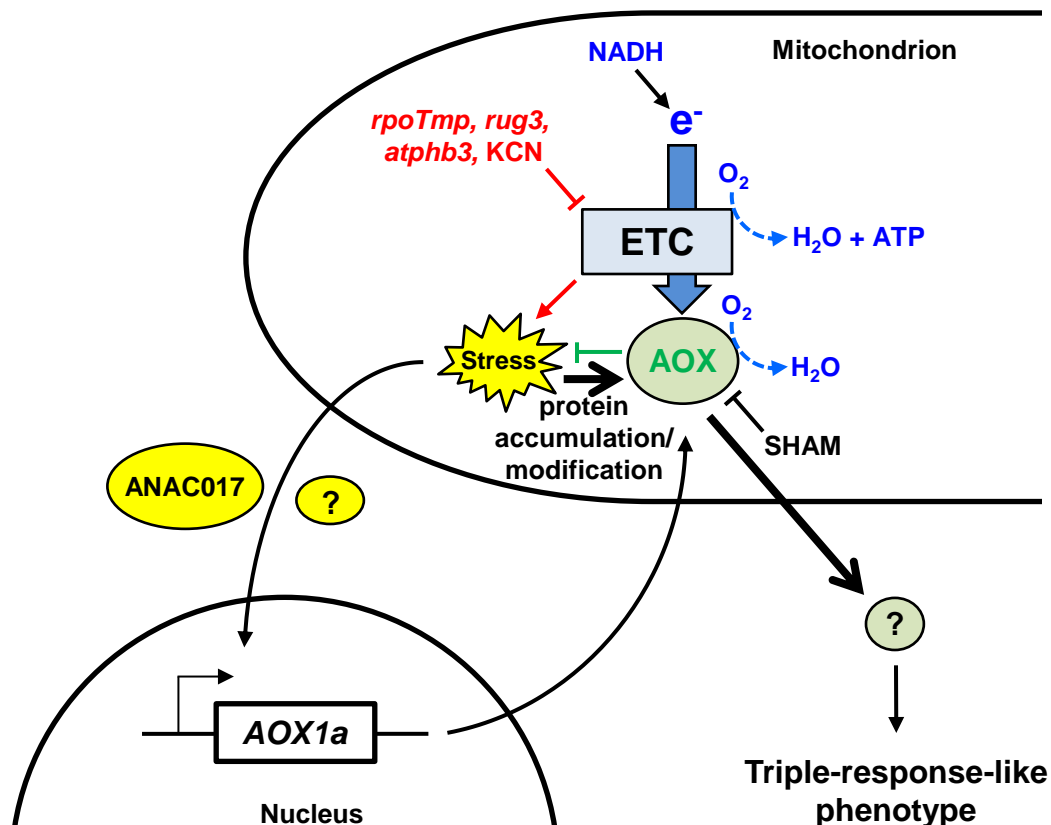


**Fig. 5 Scheme of the proposed functional link between the respiratory chain capacities (KCN-sensitive and AOX-dependent) and the skoto-morphogenic programme.** In mitochondria the KCN-sensitive transport of electrons (ETC) from NADH is used for  $O_2$  reduction and ATP production. Only a limited fraction of electrons is diverted to the AOX enzyme for reduction of  $O_2$  without concomitant ATP production. In etiolated *rpoTnp*, *rug3*, *atphb3* or KCN-treated WT plants, the KCN-sensitive electron flux is strongly decreased inducing a strong dysfunctional stress (red indication). This stress activates the canonical (ANAC017-dependent) mitochondrial retrograde pathway that activates *AOX1a* expression. It may be supported by yet unknown factors (represented by a yellow oval with question mark). Additional AOX regulation by dysfunctional stress at the level of protein accumulation and modification might be possible (thick back arrow). As ultimate effect the capacity of the AOX-dependent chain is up-regulated and more electrons can be diverted by this pathway releasing the stress (green indication). The dysfunctional stress in combination with the highly increased AOX capacity sends a signal *via* an unknown transmitter (represented by a grey circle with question mark) that triggers the formation of the triple-like-response (or parts of it).